



Calcium-handling abnormalities underlying atrial arrhythmogenesis in a Fontan operation canine model

Wan-Ping Zhou^{1,2} · Fen Li¹ · Jin-Jin Wu¹ · Ya-Nan Lu¹ · Yi-Jiao Qian¹

Received: 17 February 2018 / Accepted: 18 July 2018 / Published online: 28 August 2018
© Children's Hospital, Zhejiang University School of Medicine 2018

Abstract

Background Atrial tachyarrhythmia (AT) is a common complication in patients who have undergone a Fontan operation. In this study, we investigated whether abnormal Ca^{2+} handling contributes to the Fontan operation-related atrial arrhythmogenic substrate.

Methods Mongrel dogs were randomly assigned to sham and Fontan groups. The Fontan operation model was developed by performing an atriopulmonary anastomosis. After 14 days, an electrophysiological study was performed to evaluate the AT vulnerability. Ca^{2+} handling properties were measured by loading atrial cardiomyocytes (CMs) with fura-2 AM. The L-type Ca^{2+} ($I_{\text{Ca-L}}$) and Na^{+} - Ca^{2+} exchanger (I_{NCX}) currents of the CMs were recorded by the whole-cell patch-clamp technique. The key Ca^{2+} handling proteins expression was assessed by Western blotting.

Results The AT inducibility was higher in the Fontan group than in the sham group (85.71 vs. 14.29%, $P < 0.05$). The Fontan operation resulted in decreased Ca^{2+} transient (CaT) amplitude and sarcoplasmic reticulum (SR) Ca^{2+} content, but in enhanced diastolic intracellular Ca^{2+} concentration and SR Ca^{2+} leak in the atrial CMs. The spontaneous CaT events, triggered ectopic activity and I_{NCX} density were increased, but $I_{\text{Ca-L}}$ density was reduced in CMs from the Fontan atria (all $P < 0.05$). Additionally, the Fontan operation resulted in decreased SR Ca^{2+} ATPase expression and Cav1.2 expression, but in increased NCX1 and Ser2814-phosphorylated ryanodine receptor 2. The calmodulin-dependent protein kinase II expression and function were markedly enhanced in the Fontan atria.

Conclusion The Fontan operation caused atrial CM Ca^{2+} handling abnormalities that produced arrhythmogenic-triggered activity and increased vulnerability to AT in experimental Fontan dogs.

Keywords Atrial tachyarrhythmia · Calcium handling · Fontan operation · Triggered activity

Introduction

The Fontan operation is a well-established surgical technique used for palliation of complex cyanotic congenital heart disease such as tricuspid atresia, double-inlet ventricle, or single ventricle defect [1]. Although mortality in Fontan patients has decreased for the modified Fontan procedure, severe complications compromise the long-term outcome.

Previous studies have recognized that arrhythmia contributes to ongoing morbidity and mortality in patients with a Fontan circulation [2]. The most frequent of these is atrial tachyarrhythmia (AT), seen in 7.3–41% of Fontan patients [3–5]. However, the exact mechanisms of postoperative AT in Fontan patients are not well defined. Although atrial dilatation and surgical scars within the atrial mass induce a reentry substrate in the Fontan atria [6], there is also evidence that focal drivers and triggered activity play a role in Fontan operation-related AT [7–9]. At the cellular level, triggered activity can be caused by abnormal calcium handling [10]. However, there are no published descriptions of atrial calcium handling in Fontan patients or relevant animal models. In this study, we developed a Fontan model by creating an atriopulmonary anastomosis (APA) in canine hearts and evaluated atrial cardiomyocyte calcium handling remodeling after a Fontan operation.

✉ Fen Li
lifeng@scmc.com.cn

¹ Cardiology Department, Shanghai Children's Medical Center, Shanghai Jiaotong University School of Medicine, 1678 Dongfang Road, Pudong New Area 200127, Shanghai, China

² Cardiology Department, Children's Hospital of Soochow University, Suzhou, China

Methods

Fontan operation canine model

All animal-handling procedures followed the National Institutes of Health guidelines and were approved by the Shanghai Children's Medical Center Animals Research Ethics Committee. Adult male mongrel dogs (weighing 15–20 kg) assigned into sham and Fontan operation (Fontan) groups. After the dogs were anesthetized with zoletil (2.5 mg/kg i.v.) and xylazine (0.15 mg/kg i.v.), median sternotomy and pericardiectomy were performed to expose the hearts in both groups. In Fontan groups, the pulmonary artery was separated by blunt dissection. Subsequently, a portion of the right atrial appendage was clamped with a lateral forceps and anastomosed with a 10 mm Goretex tube (W.L. Gore & Associates, Inc. Flagstaff, AZ, USA) by end-to-side, followed by an anastomosis of another end of Goretex tube with the pulmonary artery wall without cardiopulmonary bypass. The proximal pulmonary artery was ligated (Fig. 1). The sham group underwent only thoracotomy and pericardiectomy; however, this group did not undergo right atrium (RA)-pulmonary artery (PA) connection and pulmonary valve cerclage. A surgical plane of anesthesia was maintained using propofol (2 mg/kg i.v.), and systemic

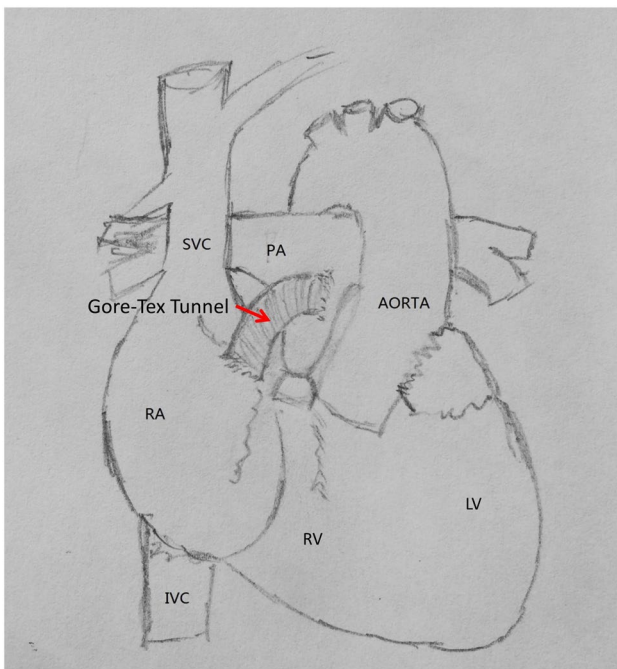


Fig. 1 The schematic figure of Fontan operation performed in this study (made by Zhou WP). The right atrium (RA) and main pulmonary artery (PA) was connected by using a 10 mm Gore-Tex Tunnel. The proximal PA was blocked to mimic pulmonary valve cerclage. SVC superior vena cava, IVC inferior vena cava, RV right ventricle, LV left ventricle

heparinization was administered continuously (1 mg/kg) throughout the surgery. Surface electrocardiograph (ECG) and blood pressure (BP) were also continuously recorded throughout the surgery. Normal saline (50–100 mL/hour) was infused to replace spontaneous fluid losses. All efforts were made to minimize suffering. A 24-hour Holter recording was performed on the first postoperative day, and normal limb-ECG was recorded daily after surgery. Echocardiography analysis was performed to assess the right atrium dimension (RAD), a puncture needle connected to a pressure transducer was used to record right atrium pressure (RAP), and pulmonary artery systolic pressure (PASP) at baseline and 14 days after surgery.

In vivo electrophysiological study

Two weeks after surgery, an open-chest electrophysiological study was performed in both groups. Briefly, dogs were anesthetized and ventilated, a median sternotomy was performed, and bipolar recording electrodes were hooked into the RA appendage (RAA). To estimate atrial tachycardia (AT) vulnerability in each dog, AT was induced with 2 seconds burst pacing for 10 times (2-ms pulses at 50 Hz, which is 4 times the threshold current) in the RAA. Prolonged AT (> 20 minutes) was terminated by direct-current electrical cardioversion, and a 20-minute rest period was allowed for cardiac electrical recovery.

Histological analysis

Heart tissue sections from RA ($n=5$ in each group) were fixed in 10% phosphate-buffered formalin and embedded in paraffin. Paraffin sections were stained with Masson trichrome to visualize collagen deposition. Fibrosis was quantified in each heart section as the average myocardial interstitial collagen volume fraction (CVF) in four random areas of the left ventricular free wall. The mean CVF for each sample was calculated.

Atrial cardiomyocytes isolation

RA cardiomyocytes were isolated as described previously [11]. Briefly, dogs were anesthetized with zoletil (2.5 mg/kg i.v.) and xylazine (0.15 mg/kg i.v.). After intra-atrial injection of heparin (10,000 U), the heart was quickly removed and placed in Tyrode solution contained (in mM): NaCl 136, KCl 5.4, MgCl₂ 1, CaCl₂ 2, NaH₂PO₄ 0.33, HEPES 5, and dextrose 10 (pH adjusted to 7.35 with NaOH). The right coronary artery was cannulated, and the RA tissue was dissected free and perfused with 1.8 mM Ca²⁺ containing Tyrode's solution (37 °C, 100% O₂). Any leak from arterial branches was ligated with silk thread to maintain adequate perfusion. Subsequently, the

tissues were perfused with Ca^{2+} -free Tyrode's solution for 5 to 10 minutes, followed by Ca^{2+} -free Tyrode's solution containing collagenase (about 0.45 mg/mL, CLS II, Worthington, Freehold, NJ, USA) plus 0.1% bovine serum albumin (Sigma, St. Louis, MO, USA) for 1 hour. Digested tissue was carefully minced and agitated, and the RA cardiomyocytes harvested. After isolation, cells were kept in KB solution (in mM): KCl 20, KH_2PO_4 10, dextrose 10, mannitol 40, L-glutamic acid 70, β -hydroxybutyric acid 10, taurine 20, EGTA 10, and 0.1% bovine serum albumin (pH adjusted to 7.3 with KOH) at 4 °C for current recordings, and in 0.2 mM Ca^{2+} containing Tyrode's solution for Ca^{2+} imaging experiments.

Measurement of cell contraction and Ca^{2+} fluorescence

Cardiomyocytes (CMs) were incubated with Fura-2-AM (5 μM) in 100 $\mu\text{mol/L}$ Pluronic F-127 and 0.5%-dimethyl sulfoxide for about 20 minutes and then superfused with 2.0 mM Ca^{2+} containing Tyrode's solution for about 20 minutes. Fura-2 was excited by the μStep Light Source system (IonOptix Corporation, Milton, MA, USA). The excitation wavelengths were 340 nm and 380 nm, and emission was measured at 510 nm. After background subtraction, the fluorescence signal ratios (F340/380) were obtained and calibrated into Ca^{2+} concentration as previously described [12, 13].

Fluorescence ratios were obtained from whole cells by dividing the 340 nm image after background subtraction by the 380 nm image after background subtraction.

Myocytes experienced the sequence of protocols as following [14]: 1) calcium transients (CaTs) were evoked by 1 Hz field stimulation in 2.0 mM Ca^{2+} Tyrode's solution at 37 °C; 2) cells were perfused with Ca^{2+} and Na^+ -free solution (in mM): 140 LiCl, 4 KCl, 1 MgCl_2 , 2 EGTA, 5 HEPES, and 10 glucose (pH adjusted to 7.4 with LiOH) to suppress the plasma membrane $\text{Na}^+/\text{Ca}^{2+}$ exchanger, and then the tetracaine-induced decrease in $[\text{Ca}^{2+}]_i$ was detected; 3) the sarcoplasmic reticulum (SR) Ca^{2+} content ($[\text{Ca}^{2+}]_{\text{SR}}$) was measured by rapidly adding 10 mM of caffeine using a solution switching device; and 4) spontaneous CaTs (SCaTs) were observed during the first 10 seconds after Ca^{2+} loading by 30 seconds periods of pacing at 2 Hz. A successful spontaneous Ca^{2+} -release event was defined as an unstimulated CaT (accompanied by cellular contraction) that reached at least 50% of the steady-state signal at 2 Hz. Cell-shortening was measured by 1 Hz field stimulation used a video edge-detector. All measurements were acquired and analyzed with IonWizard 6.2 software (IonOptix Corporation, Milton, MA, USA).

Cellular electrophysiology

Action potential (AP) was recorded with whole-cell perforated-patch methods. Borosilicate glass electrodes (1.0 mm outer diameter) had tip resistances between 2 and 4 M Ω . Pipette tips were filled with a nystatin-containing (60 $\mu\text{g/mL}$) intracellular solution. Junction potentials averaged 10.5 mV and were corrected for APs. Typical APs were recorded at 2 Hz for sequential 2-minute periods. The action potential duration (APD) was determined at 80% repolarization (APD_{80}) based on the average of five consecutive APs. As previously described [11, 15], the L-type Ca^{2+} ($I_{\text{Ca-L}}$) and $\text{Na}^+-\text{Ca}^{2+}$ exchanger (I_{NCX}) currents were recorded in CMs at 36 ± 1 °C with a whole-cell ruptured-patch configuration. Data were sampled at 5 kHz and filtered at 1 kHz. Whole cell currents were expressed as densities (pA/pF) to account for differences in cell size. Data were recorded and analyzed with Clampfit10.4 software (Axon Instruments, USA).

The extracellular solution for AP recording is normal Tyrode's solution. The pipette solution for AP recording contained (in mM): 0.1 GTP, 110 potassium aspartate, 20 KCl, 1 MgCl_2 , 5 MgATP, 10 HEPES, 5 sodium-phosphocreatine, and 0.005 EGTA (pH adjusted to 7.4 with KOH). The extracellular solution for $I_{\text{Ca-L}}$ measurement contained (in mM): 136 tetraethylammonium-chloride, 5.4 CsCl, 1 MgCl_2 , 2.0 CaCl_2 , 0.33 NaH_2PO_4 , 10 dextrose, and 5 HEPES (pH adjusted to 7.4 with CsOH). Niflumic acid (50 μM) was added to inhibit Ca^{2+} -dependent Cl^- current, and 2 mM 4-aminopyridine to suppress Ito. The pipette solution for $I_{\text{Ca-L}}$ -recording contained (in mM): 120 CsCl, 20 tetraethylammonium-chloride, 1 MgCl_2 , 10 EGTA, 5 Mg-ATP, 10 HEPES, and 0.1 Li-GTP (pH adjusted to 7.4 with CsOH). The extracellular solution for I_{NCX} contained (in mM): 140 NaCl, 2 CaCl_2 , 1 MgCl_2 , 1, 10 dextrose, 10 HEPES, 0.1 niflumic acid, and 0.005 nifedipine. The internal solution for I_{NCX} contained (in mM): 130 CsCl, 5 NaCl, 4 MgATP, and 10 HEPES (pH adjusted to 7.3 with CsOH).

Western blotting analysis

RA tissue ($n=5$ in each group) was collected and stored in tubes at about 80 °C until Western blotting analysis was performed. Western blotting was performed to determine the relative expression levels of Cav1.2, $\text{Na}^+/\text{Ca}^{2+}$ -exchanger (NCX1), total ryanodine receptor 2 (t-RyR2), Ser2814-phosphorylated RyR2 (p-RyR2), sarcoplasmic reticulum Ca^{2+} -ATPase (SERCA2a), phospholamban (PLB), total calmodulin-dependent protein kinase II (t-CaMKII), and Thr287-phosphorylated CaMKII (p-CaMKII). In this study, the protein levels were normalized to glyceraldehyde 3-phosphate dehydrogenase.

Statistical analysis

SPSS 17.0 for Windows (SPSS Inc., Chicago, IL, USA) was used for the statistical analyses. Group data are presented as mean \pm SD. Individual group-mean differences were evaluated with a Student's *t* test. Contingency analyses were measured by a χ^2 test. Two-tailed $P < 0.05$ was considered statistically significant.

Results

Fontan animal model and changes in cardiac structural

We performed a Fontan operation in 14 dogs. 10 dogs undergone Fontan operation survived 2 weeks. Table 1 shows echocardiographic parameters in both groups at baseline and 14 days after surgery. At baseline, there were no significant differences in terms of RAD, RAP, and PASP between the sham and Fontan groups (all $P > 0.05$). However, compared with the sham group, the RAD and RAP were markedly increased in the Fontan group at 14 days after surgery (all $P < 0.05$). Consistent with these results, histopathology of the heart sections showed that the average myocardial interstitial CVF was also markedly increased in the Fontan group when compared with the sham group ($P < 0.01$; Fig. 2).

Changes in AT vulnerability

In the present study, AT was elicited by burst pacing in both groups in vivo. We observed that the Fontan group displayed a higher AT inducibility than did the sham group (Fontan 85.71% vs. sham 14.29%, $P < 0.01$), indicating an increased AT vulnerability in the Fontan group (Fig. 3).

Alterations in cell-shortening and CaTs

Figure 4a, b shows representative cell-shortening recordings and steady-state CaTs at 1 Hz in each group. Compared with the sham group, the overall cell-shortening was strongly reduced in CMs in the Fontan group ($P < 0.01$) (Fig. 4c). Additionally, an increased diastolic $[Ca^{2+}]_i$ level

and a decreased CaT amplitude were found in atrial CMs in the Fontan group when compared to the sham group (all $P < 0.01$) (Fig. 4d, e).

Diastolic SR Ca^{2+} leak and SR Ca^{2+} content

As illustrated in Fig. 5a, we used the tetracaine method to directly quantify total SR Ca^{2+} leak, in which SR Ca^{2+} leak is quantified as the decrease in $[Ca^{2+}]_i$ when RyR2 channels are blocked with tetracaine in CMs perfused with 0 Na^+ and 0 Ca^{2+} bath solution. Additionally, the application of caffeine was used to assess SR Ca^{2+} content under the same conditions. The SR Ca^{2+} content was significantly decreased in Fontan cells (195.00 ± 21.65 nM, $n/N = 9/4$) versus sham cells (290.00 ± 27.39 nM, $n/N = 9/4$, $P < 0.01$). The decreased SR Ca^{2+} content in Fontan cells might be partly attributable to increased SR Ca^{2+} leak (65.00 ± 10.61 nM, $n/N = 9/4$) versus sham cells (27.89 ± 7.57 nM, $n/N = 9/4$; $P < 0.01$).

SCaTs and triggered APs

Typical recordings of SCaTs in both groups are shown in Fig. 6a. Compared with the sham group, many more SCaTs were seen in atrial CMs from the Fontan group ($P < 0.01$, Fig. 6c). Figure 6b shows whole-cell perforated-patch AP recordings immediately after 1 minute of stimulation at 2 Hz. In sham atrial CMs, triggered APs were rare, whereas triggered activity was greatly increased in Fontan CMs (Fig. 6d). These results suggested that CMs from Fontan hearts displayed an increased automaticity.

Changes in cellular electrophysiology

Figure 7 shows the typical AP recordings for both groups. The Fontan operation induced an abbreviated APD_{80} in CMs from this group when compared to that of the sham group (Fontan group 146.50 ± 14.16 ms vs. sham group 178.00 ± 13.22 ms, 12 cells per group, $P < 0.01$).

Typical I_{Ca-L} recordings from both groups are shown in Fig. 8a, b. The density of I_{Ca-L} was significantly decreased in atrial CMs from Fontan hearts when compared to atrial CMs from sham hearts (e.g., at +10 mV,

Table 1 The echocardiographic parameters at baseline and 14 days after surgery in two groups

Variables	Baseline			14 d after surgery		
	RAD (mm)	RAP (mmHg)	PASP (mmHg)	RAD (mm)	RAP (mmHg)	PASP (mmHg)
Sham ($n = 10$), mean \pm SD	13.47 ± 0.89	10.72 ± 1.58	12.42 ± 2.64	13.76 ± 0.82	11.52 ± 1.64	12.55 ± 2.72
Fontan ($n = 10$), mean \pm SD	14.08 ± 0.92	10.41 ± 1.45	12.60 ± 2.32	$17.81 \pm 0.97^{a,b}$	$18.29 \pm 1.98^{a,b}$	13.78 ± 2.24

RAD right atrium dimension, RAP right atrium pressure, PASP pulmonary artery systolic pressure, SD standard deviation. ^a $P < 0.05$ vs. respective baseline. ^b $P < 0.05$ vs. sham group

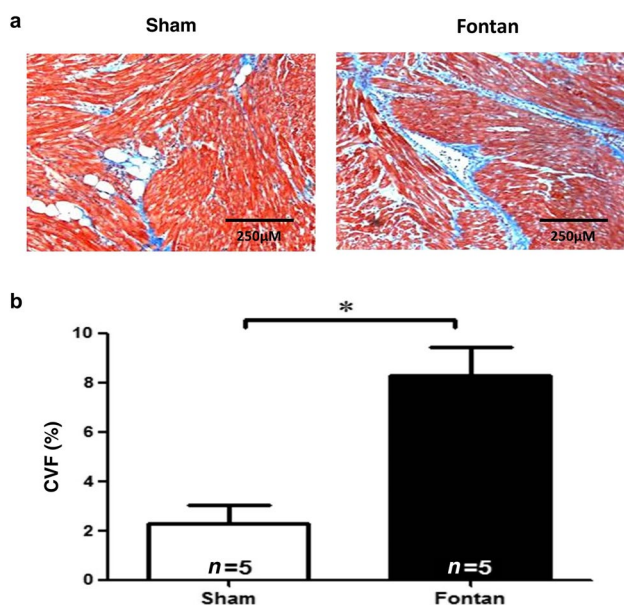


Fig. 2 Results of histological analysis in each group. **a** Masson trichrome stain shown (magnification 200 ×) in the right appendages; **b** Summarized data of myocardial fibrosis in each group. The myocardial interstitial collagen volume fraction (CVF) was significantly increased in the Fontan group versus the sham group ($*P < 0.01$)

from -5.56 ± 0.82 pA/pF in sham to -2.72 ± 0.48 pA/pF in Fontan; $n = 15$ and 12 cells, respectively; Fig. 6c). The voltage dependence of I_{Ca-L} activation and inactivation was unaffected by the Fontan operation (Fig. 6d). Activation $V_{1/2}$ averaged -2.58 (95% CI -3.15 to -2.00) mV and -4.48 (95% CI -5.04 to -3.91) mV in the sham and Fontan groups, respectively (12 cells per group, $P > 0.05$). Inactivation $V_{1/2}$ averaged -26.42 (95% CI -27.04 to

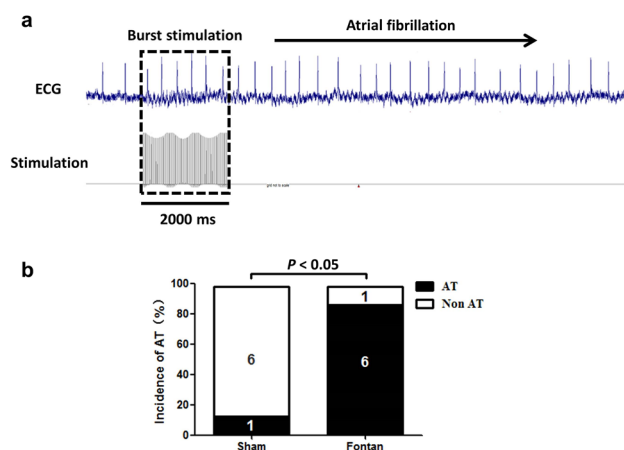


Fig. 3 Results of AT inducibility in two groups. **a** The example of atrial fibrillation elicited by Burst pacing in the Fontan group; **b** The inducibility of AT in each group. Compared with the sham group, the AT vulnerability was increased in the Fontan group ($P < 0.05$). AT atrial tachycardia, ECG electrocardiograph

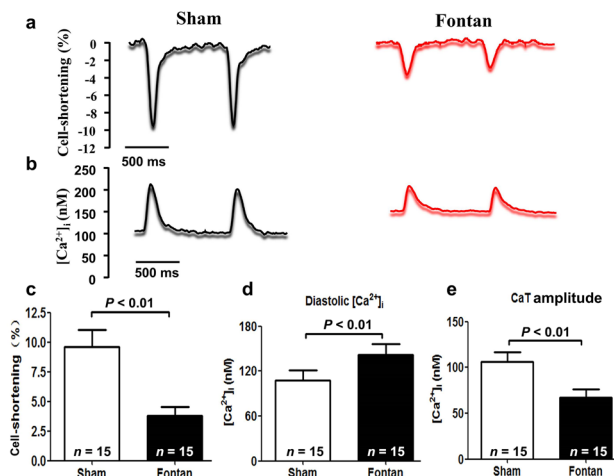


Fig. 4 Results of cell-shortening and calcium transient (CaT) in two groups. **a, b** Recordings of cell-shortening (**a**) and Ca^{2+} transients (**b**) from single sham and Fontan cardiomyocytes; **c–e** Summarized data of cell-shortening (**c**), diastolic intercellular Ca^{2+} level ($[Ca^{2+}]_i$) (**d**), and CaT amplitude (**e**) in each group. Compared with the sham group, the overall cell-shortening and CaT amplitude were reduced, but diastolic $[Ca^{2+}]_i$ was increased in atrial cardiomyocytes from the Fontan group (all $P < 0.01$)

-25.80) mV in the sham group and -27.24 (95% CI -27.96 to -26.51) mV in the Fontan group (12 cells per group, $P > 0.05$).

I_{NCX} recordings from both groups are illustrated in Fig. 9a, b. I_{NCX} was recorded as a lithium-sensitive

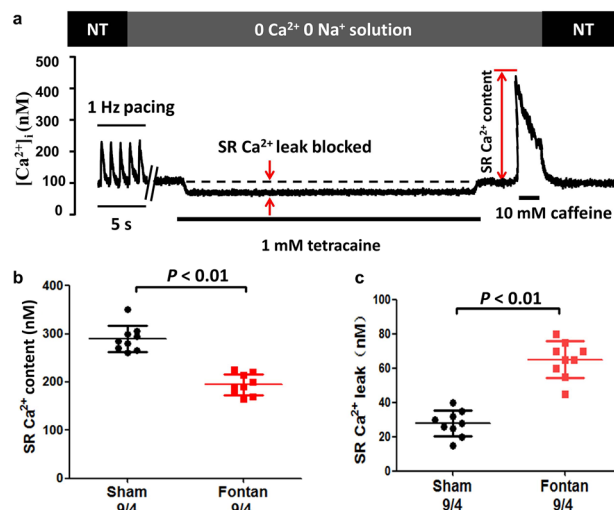


Fig. 5 Results of sarcoplasmic reticulum (SR) Ca^{2+} content and diastolic SR Ca^{2+} leak. **a** The typical recording of tetracaine-induced decrease in $[Ca^{2+}]_i$ and caffeine-induced CaT in atrial cardiomyocytes (CMs) from the sham group; **b, c** The comparisons of SR Ca^{2+} content (**b**) and diastolic SR Ca^{2+} leak (**c**) in two groups. Decreased SR Ca^{2+} content, but increased diastolic SR Ca^{2+} leak, were found in CMs from Fontan atria versus the sham group (all $P < 0.01$)

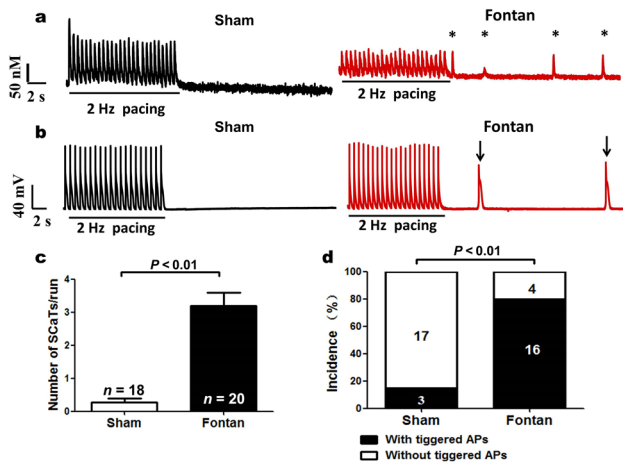


Fig. 6 **a, b** Typical recordings of spontaneous calcium transients (SCaTs) (**a**) and triggered action potential (APs) (vertical arrows) (**b**) in two groups; **c** The comparisons of SCaTs number (cell numbers provided in brackets); **d** Percentage of atrial cardiomyocytes showing triggered APs in each group (cell numbers provided in brackets)

inward current during 3000-ms repolarizing pulses. I_{NCX} density was increased in CMs from the Fontan group when compared with CMs from the sham group ($n = 10/\text{group}$, $P < 0.05$) (Fig. 7b). For example, at -120 mV, I_{NCX} averaged -2.35 ± 0.56 pA/pF and -5.21 ± 0.70 pA/pF in the sham and Fontan cells, respectively (10 cells per group, $P < 0.05$).

Changes in expression of key calcium handling proteins

The results in Figs. 6 and 7 show decreased I_{Ca-L} density and increased I_{NCX} density in CMs from the Fontan group versus the sham group. We therefore determined the protein expression of Cav1.2 and NCX1 in each group. As shown in Fig. 10a, the Fontan group displayed a decreased Cav1.2 and an increased NCX1 expression in atrial tissue compared to the sham group (all $P < 0.01$).

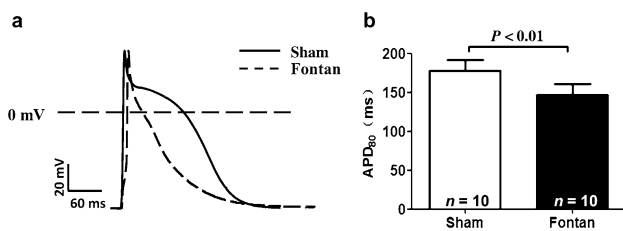


Fig. 7 **a** Typical AP waveforms of atrial cardiomyocytes obtained at 2 Hz from sham and Fontan dogs; **b** The comparisons of APD_{80} in two groups ($n = 10$ cells per group). APD_{80} was shortened in Fontan cells when compared with sham cells ($P < 0.01$). AP action potential, APD_{80} action potential duration was determined at 80% repolarization

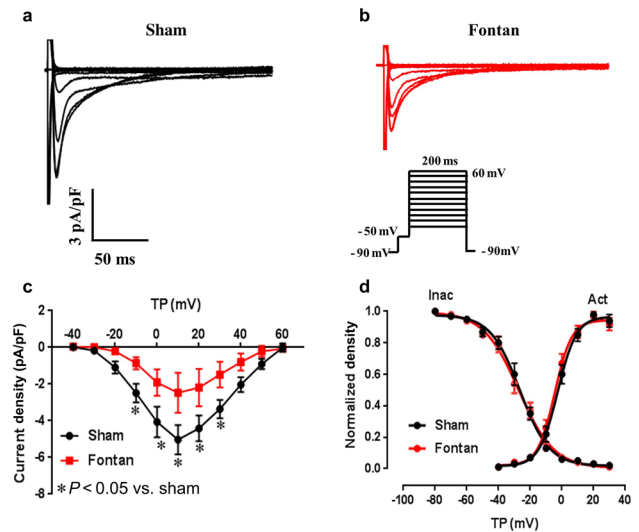


Fig. 8 **a, b** Recordings of I_{Ca-L} in sham (**a**) and Fontan (**b**) cells; **c** Mean \pm SD I_{Ca-L} density in sham and Fontan cells ($n = 15$ and 12 cells, respectively); **d** Voltage dependence of I_{Ca-L} inactivation and activation. Curves are Boltzmann fits to mean data ($n = 12$ cells per group). * $P < 0.05$ versus sham. I_{Ca-L} L-type Ca^{2+} , TP test potential, SD standard deviation

In addition, to gain insights into potential abnormalities of Ca^{2+} handling in Fontan atria, we performed Western blots to identify total and phosphorylated forms of SR calcium handling proteins. As shown in Figs. 10a, b, the protein levels of p-RyR2, t-CaMKII, and p-CaMKII were significantly increased in the Fontan group when compared with those levels in the sham group (all $P < 0.05$). Fractional RyR2 phosphorylation (Ser2814-p-RyR2 to t-RyR2) and fractional CaMKII autophosphorylation (Thr287-p-CaMKII to t-CaMKII) were also markedly

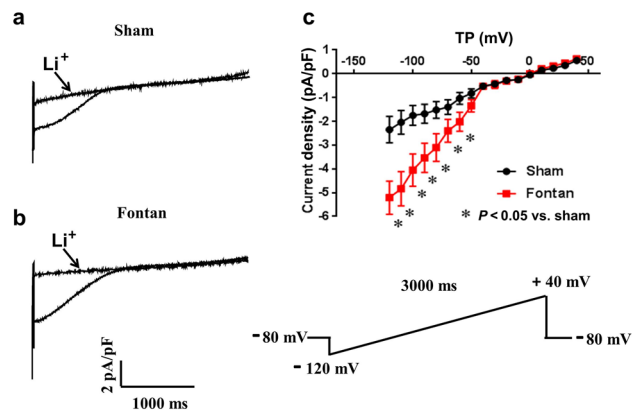


Fig. 9 **a, b** Recordings of NCX current in sham (**a**) and Fontan (**b**) cells. **c** Mean \pm SD NCX current density in sham and Fontan cells ($n = 12$ cells per group). * $P < 0.05$ versus sham. TP test potential, SD standard deviation, NCX Na^+/Ca^{2+} -exchanger

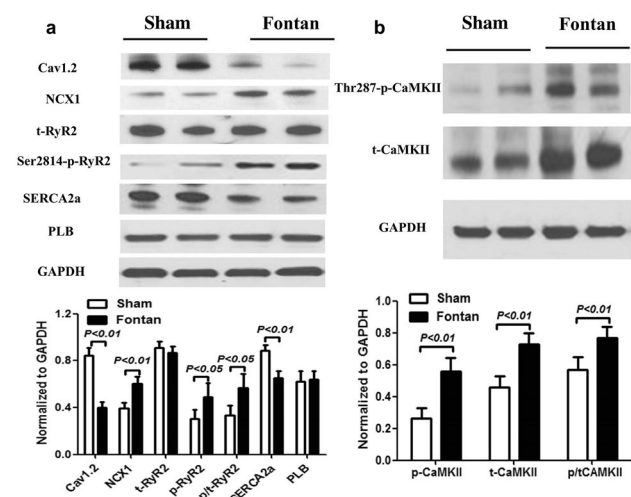


Fig. 10 Results of key Ca^{2+} -handling and -regulatory proteins expression in each group. **a** Top: representative Western blot analyses of key Ca^{2+} -handling proteins. Bottom: mean \pm SD protein-band intensities normalized to GAPDH ($n=5$ atria per group); **b** Top: representative Western blot analyses of CaMKII and Thr287-p-CaMKII (autophosphorylated). Bottom: mean \pm SD protein-band intensities normalized to GAPDH ($n=5$ atria per group). *NCX1* $\text{Na}^+/\text{Ca}^{2+}$ -exchanger, *RyR2* ryanodine receptor 2, *SERCA2a* sarcoplasmic reticulum Ca^{2+} -ATPase, *PLB* phospholamban, *CaMKII* calmodulin-dependent protein kinase II, *GAPDH* reduced glyceraldehyde-phosphate dehydrogenase

increased in Fontan atria versus sham atria (all $P < 0.05$). However, SERCA2a expression was markedly decreased in the Fontan group versus the sham group ($P < 0.01$). The expression of t-RyR2 and PLB was similar in Fontan and sham atria.

Discussion

Main finding

In the present study, we evaluated the atrial calcium handling and arrhythmogenesis in a Fontan canine model and found that: 1) atrial Ca^{2+} handling is significantly disturbed in dogs that have undergone APA, including increased diastolic $[\text{Ca}^{2+}]_i$ and Ca^{2+} leak, decreased CaT amplitude, and depletion of SR Ca^{2+} content; 2) I_{NCX} was increased but $I_{\text{Ca-L}}$ was decreased in atrial cardiomyocytes from Fontan dogs; 3) the expression of NCX1, p-RyR2, CaMKII, and p-CaMKII was markedly increased, while Cav1.2 and SERCA2a expression were significantly decreased, in Fontan atria; 4) there was increased susceptibility to spontaneous Ca^{2+} -release events and triggered activity in atrial cardiomyocytes in Fontan dogs; and 5) there was increased AT vulnerability in Fontan dogs.

The Fontan canine model

The exact mechanisms of postoperative AT in Fontan patients have not been systematically studied because of the absence of animal models. Since atriopulmonary connection is the classical procedure to create a Fontan circuit in clinical practice, we developed a Fontan canine model through APA surgery. Elevated right atrial pressure and progressive RA dilation are commonly seen in Fontan patients [16]. Additionally, impaired atrial mechanics were also found in patients after APC Fontan surgery [17]. In this study, our echocardiographic results showed RAD and RAP were markedly increased in canines at 14 days after APA surgery. In the cellular study, we observed a strongly reduced cell-shortening of Fontan atrial myocytes. These results indicated that the Fontan circulation was successfully simulated in our Fontan canine model. Furthermore, the incidence of AT was also increased in this Fontan canine model. Therefore, our Fontan canine model can be used to explore the mechanisms of AT after a Fontan operation.

CaMKII-dependent phosphorylation of RyR2 and spontaneous Ca^{2+} -release events in Fontan atrial myocytes

RyR2 is the major SR Ca^{2+} release channel required for excitation–contraction coupling in cardiomyocytes [18]. During systole, RyRs are activated by Ca^{2+} influx via adjacent L-type Ca^{2+} channels, and subsequently trigger a much larger Ca^{2+} efflux from SR [19]. By contrast, due to the finite open rate of RyRs, the diastolic SR Ca^{2+} release is rare under normal conditions. However, under disease conditions, enhanced RyR2 activity could promote Ca^{2+} release from SR in a resting period, which is known as diastolic SR Ca^{2+} leak, and finally induce spontaneous Ca^{2+} -release events in cardiomyocytes [20]. The activity of RyR2 is not only modulated by SR Ca^{2+} content but also affected by phosphorylation, s-nitrosylation, or redox mechanisms [18, 21].

In this study, the RyR2 hyperphosphorylation at the site of Ser²⁸¹⁴ and increased expression of p-CaMKII and CaMKII were found in Fontan atrial myocytes. CaMKII is a multifunction serine-threonine kinase that is abundantly expressed in the myocardium. Previous studies found that RyR2 phosphorylated by CaMKII at Ser²⁸¹⁴ could activate the RyR2s to open, which is independent of the SR Ca^{2+} content, and hence to increase the diastolic SR Ca^{2+} leak [22, 23]. Thus, although the SR Ca^{2+} content was decreased in Fontan cells, the increased RyR2 activity could stem from RyR2 hyperphosphorylated by CaMKII. The CaMKII-dependent phosphorylation of RyR2 might play an important role in the spontaneous Ca^{2+} -release events in cardiomyocytes from Fontan atria.

Trigger activity and AT in Fontan atria

Enhanced or abnormal impulse generation (e.g., focal activity) and conduction disturbances (e.g., reentry) are two major mechanisms responsible for cardiac arrhythmias.

In Fontan atria, atrial dilatation and surgical scars favor AT by promoting reentry. However, focal trigger activity may also be involved in Fontan operation-related AT. Correa et al. [7] identified eight focal ATs in five patients by using activation mapping. In a patient with Fontan palliation, two triggers were identified that initiated atrial fibrillation from the superior vena cava and the right atrium [8]. Consistent with these results, we also observed repetitive trigger activity in Fontan atrial myocytes.

Repetitive triggered activity not only can provide focal drivers that maintain AT, but also can produce bursts of rapid atrial activation that initiate a reentrant circuit in vulnerable substrates [10, 24]. In this study, our results revealed potential mechanisms underlying the Ca^{2+} handling abnormalities that cause atrial triggered activity in canine undergone Fontan operation. The central abnormality that we observed is diastolic $[\text{Ca}^{2+}]_i$ overload, likely resulting from two primary mechanisms: 1) increased diastolic Ca^{2+} leak via RyR2 and 2) decreased SERCA2a-mediated Ca^{2+} uptake due to downregulated SERCA2a expression. Increased diastolic $[\text{Ca}^{2+}]_i$ could activate I_{NCX} , which exchanges each Ca^{2+} ion for three Na^+ ions, producing a depolarizing inward current that manifests as delayed afterdepolarization, which can cause a triggered AP [25]. Moreover, we also found upregulated NCX1 expression in Fontan atria, which might be another mechanism of increased I_{NCX} in Fontan atrial myocytes.

Other mechanisms of AT in Fontan atria

Atrial fibrosis is an important contributor to AT-related reentry substrate [26]. In this study, we found increased myocardial interstitial CVF in the Fontan group, indicating obvious atrial fibrosis in Fontan atria. It remains controversial whether patients develop atrial fibrosis due to Fontan surgery. Wolf et al. evaluated the atrial remodeling in a predominantly pediatric cohort of Fontan patients who died shortly after surgery (mean 1.7 years after surgery). They found that the amount of atrial fibrosis in Fontan patients was similar to patients with a normal heart [27]. By contrast, extensive low-voltage areas (bipolar voltage ≤ 0.5 mV), which is the electroanatomic correlate for atrial fibrosis, has been shown to cover 38–44% of RA surface area in older Fontan patients (mean 18–22 years after surgery) with ATs [28, 29]. Thus, it is possible that with increasing age and time since surgery, progressive atrial fibrosis might emerge in Fontan atria, thereby providing a substrate for ATs.

We also observed decreased APD in Fontan atrial myocytes, which is an important hallmark of atrial electrical remodeling. It is proposed that changes in APD are

associated with altered ion channel function. Our results showed a reduction in $I_{\text{Ca-L}}$ of Fontan atrial myocytes, which could shorten APD in Fontan atria. In addition, there is evidence that atrial electrical remodeling can underlie atrial arrhythmogenesis by promoting reentry [25, 26]. Therefore, atrial electrical remodeling might be another mechanism of AT in Fontan canines.

Discussion

There are several limitations to the present study. Firstly, atrial electrical remodeling was found in Fontan dogs. We evaluated only the changes of the L-type Ca^{2+} channel. However, whether other ion channels, especially potassium currents, were involved in the atrial electrical remodeling of Fontan canines is still unknown. Secondly, although we found that abnormal Ca^{2+} handling might promote AT after Fontan operation, we did not provide any therapeutic intervention to our Fontan dogs. Further investigation is needed to assess the effect of Ca^{2+} handling restoration on post-operative AT in Fontan dogs. Thirdly, the sham operation should include an atriotomy. Finally, atriopulmonary Fontan is not used in clinical today, and this study only can be used to suggest the mechanism of arrhythmogenesis in the post-operative timeframe due to the short observation time. It is better to study the role of calcium handling abnormalities in later atrial arrhythmogenesis at 2 and at 12 months after operation in the future.

In conclusion, the present study demonstrates abnormal atrial cardiomyocyte Ca^{2+} handling, enhanced triggered activity, and increased AT vulnerability in dogs that underwent a Fontan operation. Our data suggest that cellular Ca^{2+} handling abnormalities might contribute to Fontan operation-related atrial arrhythmogenic substrate.

Author contributions WPZ designed the study, recorded the ion currents and measured cell contraction and Ca^{2+} fluorescence, and wrote the paper. FL designed the study. JJW did in vivo electrophysiological study. YNL performed the procedures of Fontan operation. YJQ was involved in Western blotting and histological analysis. All authors have read and approved the final manuscript.

Funding This work was supported by the National Natural Science Foundation of China (no. 81870248, 81300138), Scientific Research Program of Shanghai Science and Technology Commission (no. 13430721700) and the Jiangsu Provincial Medical Youth Talent (QNRC2016761).

Compliance with ethical standards

Ethical approval All animal-handling procedures followed the National Institutes of Health guidelines and were approved by the Shanghai Children's Medical Center Animals Research Ethics Committee. No financial or nonfinancial benefits have been received or will be received from any party related directly or indirectly to the subject of this article.

Conflict of interest None declared.

References

- Fontan F, Baudet E. Surgical repair of tricuspid atresia. *Thorax*. 1971;26:240–8.
- Giannakoulas G, Dimopoulos K, Yuksel S, Inuzuka R, Pijuan-Domenech A, Hussain W, et al. Atrial tachyarrhythmias late after Fontan operation are related to increase in mortality and hospitalization. *Int J Cardiol*. 2012;157:221–6.
- Stephenson EA, Lu M, Berul CI, Etheridge SP, Idriss SF, Margossian R, et al. Arrhythmias in a contemporary Fontan cohort: prevalence and clinical associations in a multicenter cross-sectional study. *J Am Coll Cardiol*. 2010;56:890–6.
- Ghai A, Harris L, Harrison DA, Webb GD, Siu SC. Outcomes of late atrial tachyarrhythmias in adults after the Fontan operation. *J Am Coll Cardiol*. 2001;37:585–92.
- Gelatt M, Hamilton RM, McCrindle BW, Gow RM, Williams WG, Trusler GA, et al. Risk factors for atrial tachyarrhythmias after the Fontan operation. *J Am Coll Cardiol*. 1994;24:1735–41.
- Clift P, Celermajer D. Managing adult Fontan patients: where do we stand? *Eur Respir Rev*. 2016;25:438–50.
- Correa R, Sherwin ED, Kovach J, Mah DY, Alexander ME, Cecchin F, et al. Mechanism and ablation of arrhythmia following total cavopulmonary connection. *Circ Arrhythm Electrophysiol*. 2015;8:318–25.
- Ruckdeschel ES, Kay J, Sauer WH, Nguyen DT. Atrial fibrillation ablation without pulmonary vein isolation in a patient with Fontan palliation. *Cardiac Electrophysiol Clin*. 2016;8:161–4.
- de Groot NM, Zeppenfeld K, Wijffels MC, Chan WK, Blom NA, Van der Wall EE, et al. Ablation of focal atrial arrhythmia in patients with congenital heart defects after surgery: role of circumscribed areas with heterogeneous conduction. *Heart Rhythm*. 2006;3:526–35.
- Dobrev D, Wehrens XH. Calcium-mediated cellular triggered activity in atrial fibrillation. *J Physiol*. 2017;595:4001–8.
- Nishida K, Qi XY, Wakili R, Comtois P, Chartier D, Harada M, et al. Mechanisms of atrial tachyarrhythmias associated with coronary artery occlusion in a chronic canine model. *Circulation*. 2011;123:137–46.
- Sipido KR, Callewaert G. How to measure intracellular $[Ca^{2+}]$ in single cardiac cells with fura-2 or indo-1. *Cardiovasc Res*. 1995;29:717–26.
- Meng D, Feng L, Chen XJ, Yang D, Zhang JN. Trimetazidine improved Ca^{2+} handling in isoprenaline-mediated myocardial injury of rats. *Exp Physiol*. 2006;91:591–601.
- Voigt N, Heijman J, Wang Q, Chiang DY, Li N, Karck M, et al. Cellular and molecular mechanisms of atrial arrhythmogenesis in patients with paroxysmal atrial fibrillation. *Circulation*. 2014;129:145–56.
- Cha TJ, Ehrlich JR, Zhang L, Shi YF, Tardif JC, Leung TK, et al. Dissociation between ionic remodeling and ability to sustain atrial fibrillation during recovery from experimental congestive heart failure. *Circulation*. 2004;109:412–8.
- Izumi G, Senzaki H, Takeda A, Yamazawa H, Takei K, Furukawa T, et al. Significance of right atrial tension for the development of complications in patients after atriopulmonary connection Fontan procedure: potential indicator for Fontan conversion. *Heart Vessels*. 2017;32:850–5.
- Li SJ, Wong SJ, Cheung YF. Atrial and ventricular mechanics in patients after Fontan-type procedures: atriopulmonary connection versus extracardiac conduit. *J Am Soc Echocardiogr*. 2014;27:666–74.
- Guerrero-Hernández A, Ávila G, Rueda A. Ryanodine receptors as leak channels. *Eur J Pharmacol*. 2014;739:26–38.
- Bers DM. Cardiac excitation–contraction coupling. *Nature*. 2002;415:198–205.
- Sobie EA, Guatimosim S, Gómez-Viquez L, Song LS, Hartmann H, Jafri MS, et al. The Ca^{2+} leak paradox and “rogue ryanodine receptors”: SR Ca^{2+} efflux theory and practice. *Prog Biophys Mol Biol*. 2006;90:172–85.
- Bers DM. Macromolecular complexes regulating cardiac ryanodine receptor function. *J Mol Cell Cardiol*. 2004;37:417–29.
- Bers DM, Despa S, Bossuyt J. Regulation of Ca^{2+} and Na^{+} in normal and failing cardiac myocytes. *Ann N Y Acad Sci*. 2006;1080:165–77.
- Shannon TR, Pogwizd SM, Bers DM. Elevated sarcoplasmic reticulum Ca^{2+} leak in intact ventricular myocytes from rabbits in heart failure. *Circ Res*. 2003;93:592–4.
- Yeh YH, Wakili R, Qi XY, Chartier D, Boknik P, Käab S, et al. Calcium-handling abnormalities underlying atrial arrhythmogenesis and contractile dysfunction in dogs with congestive heart failure. *Circ Arrhythm Electrophysiol*. 2008;1:93–102.
- Heijman J, Voigt N, Nattel S, Dobrev D. Cellular and molecular electrophysiology of atrial fibrillation initiation, maintenance, and progression. *Circ Res*. 2014;114:1483–99.
- Andrade J, Khairy P, Dobrev D, Nattel S. The clinical profile and pathophysiology of atrial fibrillation. *Circ Res*. 2014;114:1453–68.
- Wolf CM, Seslar SP, den Boer K, Juraszek AL, McGowan FX, Cowan DB, et al. Atrial remodeling after the Fontan operation. *Am J Cardiol*. 2009;104:1737–42.
- Abrams DJ, Earley MJ, Sporton SC, Kistler PM, Gatzoulis MA, Mullen MJ, et al. Comparison of noncontact and electroanatomic mapping to identify scar and arrhythmia late after the Fontan procedure. *Circulation*. 2007;115:1738–46.
- Yap SC, Harris L, Downar E, Nanthakumar K, Silversides CK, Chauhan VS. Evolving electroanatomic substrate and intra-atrial reentrant tachycardia late after Fontan surgery. *J Cardiovasc Electrophysiol*. 2012;23:339–45.